

## EFFECT OF SULFIDE IONS ON THE CORROSION BEHAVIOUR OF MILD STEEL IN ACETATE BUFFER

Hyman H. REIHAN, Said A. SALIH, Hassan EL-DALEY and Ahmed G. GAD-ALLAH

*Department of Chemistry, Faculty of Science, Cairo University Giza, Egypt*

Received August 7, 1991

Accepted March 6, 1992

The corrosion behaviour of mild steel was investigated in acidic acetate buffer solutions using impedance and potential measurements. It was found that there are two dissolution rates resulting from the duplex nature of the formed oxides. The dissolution rates were found to depend on the dissolving acetate buffer solution pH and the dissolution temperature. In all cases, the film thickness was found to decrease with time of corrosion according to the relation  $C_m^{-1} = (C_m^0)^{-1} - k_d t^{1/2}$ . It was found that addition of sulfide ions increases the dissolution rate and increases the rate of hydrogen evolution reaction but does not affect the mechanism of cathodic process. The role of sulfide ions on the corrosion behaviour of steel in acetate buffer solutions is revealed by the complex plane impedance analysis.

Although the corrosion behaviour of iron has been extensively studied in neutral and alkaline media especially in borate ones<sup>1-10</sup>, the effect of sulfide ions on such behaviour seems to have received little attention. The corrosion behaviour of many metals, such as iron in sulfide ions containing environment, forms the bases of many industries problems of considerable significance.

However, little is also known about fundamental processes occurring on the iron surface in acetate buffer solutions in the absence of sulfide ions<sup>11-16</sup>. The present work concerns with the study of the corrosion behaviour iron in acetate buffer solutions over the pH range 3.72 – 5.57 in the absence and presence of sulfide ions by impedance and potential measurements. The former method may clarify the role of sulfide ions on the corrosion behaviour of iron in acidic buffer solutions.

### EXPERIMENTAL

The electrode preparation, electrolytic cell and electric circuit were described elsewhere<sup>17,18</sup>. All solutions were prepared from analytical grade chemicals and triply distilled water. The acidic buffer solutions (pH 3.72 – 5.57) were prepared by adding 0.2 M sodium acetate to 10 ml of 0.2 M acetic acid to the desired pH (ref.<sup>19</sup>). Mild steel electrodes were manufactured in Company of Steel and Iron, Helwan, Egypt; with the following composition: 0.015% C, 0.005% Mn, 0.017% S, 0.022% P.

Before each experiment, the electrode was abraded using successively finer grades of metallographic emery papers down to 4/0 till the metal acquired a mirror bright surface<sup>20</sup>, rinsed with triply distilled water and transferred to acetate buffer solution. Capacitance  $C_m$  and resistance  $R_m$  were measured at 1 kHz, and

the electrode potential  $E$  was measured relative to a saturated calomel electrode (SCE). All experiments were carried out in a double-walled electrically controlled air thermostat at the desired temperature ( $\pm 0.2$  °C).

## RESULTS AND DISCUSSION

During the dissolution process, the electrode potential was found to shift towards more negative values. As shown in Fig. 1, the decrease in the resistance  $R_m$  with time appears to be consistent with that of the electrode potential  $E$ . It was found that the reciprocal capacitance  $C_m^{-1}$  of steel electrode decreases with time too (Fig. 2). Assuming that the dielectric constant of the passive layer is almost invariable,  $C_m^{-1}$  is proportional to the layer thickness<sup>21,22</sup>, and hence the decrease in  $C_m^{-1}$  reflects the dissolution behaviour of steel in this buffer solution.

### *Effect of Sulfide Ion on the Dissolution Behaviour*

It is obvious from Fig. 2 that the reciprocal capacitance decreases linearly with the square root of time in acetate buffer solutions indicating oxide thinning according to the equation<sup>23</sup>

$$C_m^{-1} = (C_m^0)^{-1} - k_d t^{1/2}, \quad (1)$$

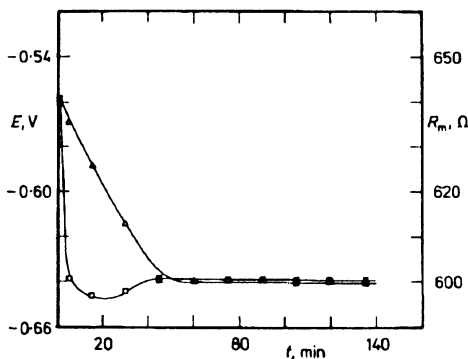


FIG. 1  
Variation of  $E$  ( $\blacktriangle$ ) and  $R_m$  ( $\triangle$ ) of steel electrode with time at pH 3.72 and 30 °C

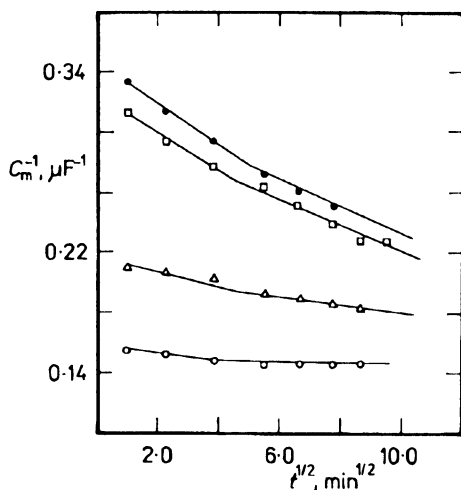


FIG. 2  
Variation of the reciprocal capacitance  $C_m^{-1}$  of steel electrode with the square root of time at 30 °C and different pH values:  $\bullet$  3.72,  $\square$  4.27,  $\circ$  4.80,  $\circ$  5.57

where  $(C_m^0)^{-1}$  is the reciprocal capacitance at zero time and  $k_d$  is the dissolution rate constant. The values of  $k_d$  in different pH's are given in Table I. It has become clear that there are two different dissolution rates of the passive film formed on the electrode surface reflecting the duplex nature of the passive film. It has been known that the passive oxide film formed on iron consists of an outer layer of  $\gamma\text{-Fe}_2\text{O}_3$  and of an inner layer of  $\text{Fe}_3\text{O}_4$  (refs<sup>2,24</sup>). The dissolution rate of the outer layer is higher than that of the inner one. This indicates that once  $\gamma\text{-Fe}_2\text{O}_3$  was consumed by rapid dissolution in an acid solution, it was followed by slow dissolution of the magnetite layer and surface activation.

Figure 3 shows the variation of the reciprocal capacitance with the square root of time in the presence of sulfide ions. As it can be shown, the dissolution occurs in the oxide film formed on the electrode surface. The effect of sulfide ions on the dissolution rate becomes pronounced at concentrations higher than  $10^{-3}$  mol  $\text{l}^{-1}$ , and the relative dissolution rate can be computed using the following equation

$$\tilde{v} = \frac{C_{mi}^{-1} - C_{mf}^{-1}}{C_{mi}^{-1}} \frac{1}{t} \quad (2)$$

where  $C_{mi}^{-1}$  and  $C_{mf}^{-1}$  are the measured reciprocal capacitances at the beginning and after attainment of steady state, respectively and  $t$  is time needed to reach the steady state

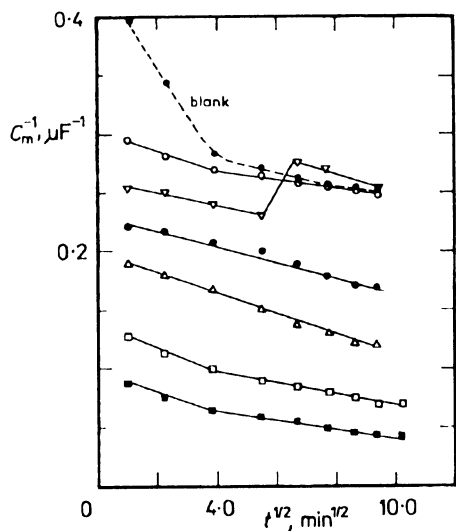


FIG. 3

Variation of the reciprocal capacitance  $C_m^{-1}$  of steel electrode with the square root of time at  $30^\circ\text{C}$ , pH 3.72 and different concentrations of sulfide ions (mol  $\text{l}^{-1}$ ):  $\nabla$   $1 \cdot 10^{-4}$ ,  $\circ$   $1 \cdot 10^{-3}$ ,  $\bullet$   $5 \cdot 10^{-3}$ ,  $\Delta$   $1 \cdot 10^{-2}$ ,  $\square$   $5 \cdot 10^{-2}$ ,  $\blacksquare$   $1 \cdot 10^{-1}$

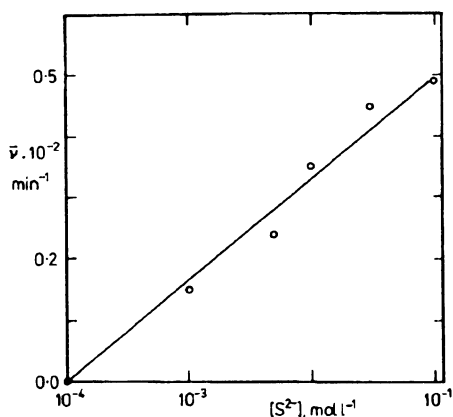


FIG. 4

The dependence of the relative dissolution rate on the logarithm of sulfide ion concentration at pH 3.72 and  $30^\circ\text{C}$

values. As it can be seen from Fig. 4, the dependence of the relative dissolution rate  $\tilde{v}$  on the logarithm of sulfide ion concentration fits the relation

$$\tilde{v} = a + b \log [S^{2-}] , \quad (3)$$

where  $a$  and  $b$  are constants depending on the medium composition.

The effect of the sulfide ion concentration on the rate of hydrogen evolution is illustrated in Fig. 5. It is shown that sulfide ions do not affect the mechanism of the cathodic process, but increase the rate of hydrogen evolution reaction.

### Complex Plane Analysis

Complex plane analysis has been accepted as a powerful tool in passivity studies<sup>25-28</sup> and analysis of electrode kinetics. The passive layer ability to retard the charge carrier flow (i.e. to impede the rate of electrochemical reaction) may be elucidated from the relation between the real and imaginary parts of electrode impedance. For this purpose,

TABLE I  
Dissolution rate constants of steel electrode at 30 °C

pH	$(k_d)_1$ $10^{-3} \mu l^{-1} \min^{-1/2}$	$(k_d)_2$ $10^{-3} \mu l^{-1} \min^{-1/2}$
3.72	14.0	10.00
4.27	12.5	8.66
4.80	5.0	3.07
5.57	2.8	-

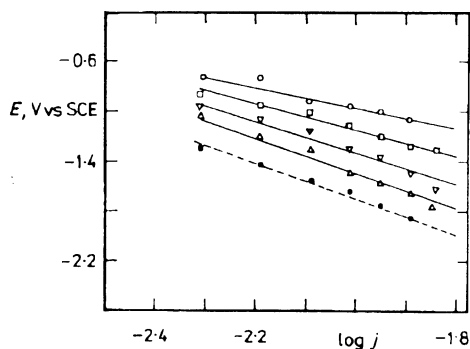


FIG. 5  
The effect of  $S^{2-}$  on the hydrogen evolution current density  $j$  (in  $A \text{ cm}^{-2}$ ) on steel at pH 3.72 and 30 °C. Sulfide concentration ( $\text{mol l}^{-1}$ ): ●  $1 \cdot 10^{-1}$ , ▲  $1 \cdot 10^{-3}$ , ▼  $5 \cdot 10^{-3}$ , ▽  $1 \cdot 10^{-2}$ , ○  $1 \cdot 10^{-1}$

the frequency effect on the two vector components of electrode impedance  $C_m$  and  $R_m$  was studied in the pH range 3.72 – 5.57 in the absence and presence of sulfide ions, after attainment of steady state values. Figure 6 illustrates the impedance spectra at different pH values. The line slopes give indications about the insulating properties of the passive layer<sup>29</sup> and the dielectric loss angle  $\delta$  ( $\delta = 90 - \Theta$ ) (ref.<sup>30</sup>). The slopes,  $\Theta$  and dielectric loss angle  $\delta$  are given in Table II including the effect of sulfide ion concentration on the complex plane analysis of steel electrode at pH 3.72. It is obvious from these data that the insulating properties of the passive layers deteriorate as the acidity increases. Also, with increasing sulfide ion concentration, the slope and phase shift  $\Theta$  decrease and, at the same time, the dielectric loss angle  $\delta$  increases.

TABLE II

Variation of the loss angle  $\delta$ , phase shift  $\Theta$ , and the solution resistance  $R$  of steel electrode in acetate buffer solutions in the absence and presence of  $S^{2-}$

pH	$[S^{2-}]$ mol l <sup>-1</sup>	Slope	$\Theta$ , °	$\delta$ , °	$R$ , $\Omega$
3.72	–	4.46	77.4	12.6	540
	0.010	4.29	76.9	13.1	357
	0.005	3.70	74.9	15.1	443
	0.001	1.43	55.0	35.0	600
4.27	–	4.27	78.7	11.3	230
4.80	–	5.50	79.7	10.3	165
5.57	–	6.60	81.4	8.6	90

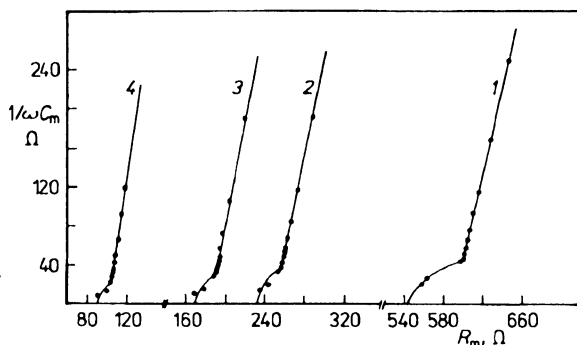


Fig. 6

Complex plane impedance of a steel electrode after 3 h immersion in solutions of different pH at 30 °C. pH of solutions: 1 3.72, 2 4.27, 3 4.8, 4 5.57

### Effect of Temperature on the Dissolution Behaviour

The variation of  $C_m^{-1}$  with the square root of time at different temperatures is shown in Fig. 7. As it can be seen,  $C_m^{-1}$  decreases as the temperature increases. At low temperatures ( $\leq 293$  K), the rate of dissolution is very low (see Table III). As the temperature increases, the rate of dissolution increases. For each temperature in all measurements, an inflection in the  $C_m^{-1}$  versus  $t^{1/2}$  is obtained. The inflection time decreases as the temperature increases. The relation between the rate of dissolution, represented by  $dC_m^{-1}/dt^{1/2}$ , and  $1/T$  gives straight lines (Arrhenius plot), which correspond to the first and the second segments of the  $C_m^{-1}$  versus  $t^{1/2}$  relation at different temperatures (Fig. 8). From the slopes of these lines the activation energy of the dissolution process may be calculated as

$$-R \, d \ln (k_d)_1 / d (1/T) = 15.9 \, \text{kJ mol}^{-1}$$

TABLE III  
Variation of the dissolution rate with temperature in acetate buffer at pH 3.72

$T, \text{K}$	$(k_d)_1$ $10^{-3} \, \mu\text{F}^{-1} \text{min}^{-1/2}$	$(k_d)_2$ $10^{-3} \, \mu\text{F}^{-1} \text{min}^{-1/2}$
293	9.0	—
303	11.0	2.7
313	13.8	6.0
323	17.6	13.6

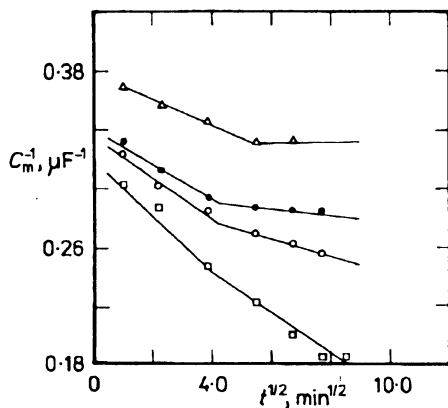


FIG. 7  
Variation of the reciprocal capacitance  $C_m^{-1}$  of steel electrode with the square root of time at pH 3.72 and different temperatures ( $^{\circ}\text{C}$ ):  $\Delta$  20,  $\bullet$  30,  $\circ$  40,  $\square$  50

and

$$-R \, d \ln (k_d)_2 / d (1/T) = 65.8 \text{ kJ mol}^{-1}.$$

The two values obtained from the two segments (cf. Fig. 8) are rather different. This indicates that the oxide films formed are different in nature, which needs further investigation.

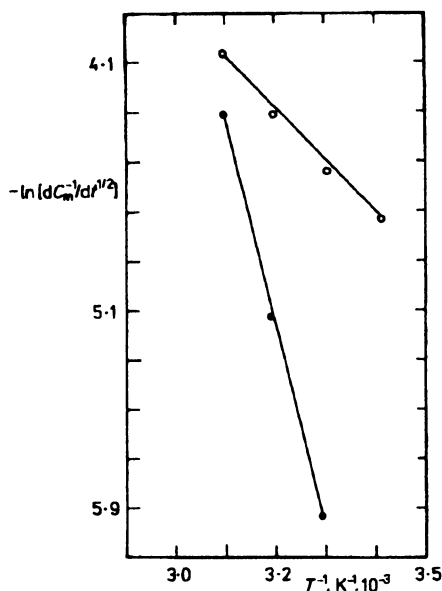


FIG. 8  
Variation of dissolution rates of steel electrodes with the reciprocal absolute temperature  $T^{-1}$  at pH 3.72: ○  $(k_d)_1$ , ●  $(k_d)_2$

The authors would like to thank Professor M. S. El-Basoumy for continuous support and fruitful discussion.

## REFERENCES

1. Stockbridge C. D., Sewell P. B., Cohen M.: *J. Electrochem. Soc.* **108**, 928 (1961).
2. Nagayama M., Cohen M.: *J. Electrochem. Soc.* **109**, 781 (1962).
3. Nagayama M., Cohen M.: *J. Electrochem. Soc.* **110**, 670 (1963).
4. Sato N., Kudo K., Noda T.: *Corros. Sci.* **10**, 785 (1970).
5. Chen C. T., Cahan B. D.: *J. Electrochem. Soc.* **129**, 17 (1982).
6. Szklarska-Smialowska Z., Kozłowski W.: *J. Electrochem. Soc.* **131**, 499 (1984).
7. Goetz R., Mitchell D. F., MacDougall B., Graham M. J.: *J. Electrochem. Soc.* **134**, 535 (1987).
8. Bardwell J. A., MacDougall B., Graham M. J.: *J. Electrochem. Soc.* **135**, 413 (1988).
9. Wroblowa H., Brusie V., Bockris J. O'M.: *J. Phys. Chem.* **75**, 2823 (1971).
10. Vela M. E., Vilche J. R., Arvia A. J.: *J. Appl. Electrochem.* **16**, 490 (1986).
11. Vdovenko I. D., Anikina N. S.: *Zash. Met.* **10**, 157 (1974).

12. Anikina N. S., Vdovenko I. D.: *Zash. Met.* *11*, 607 (1975).
13. Christiansen K. A., Heg H., Michelsen K., Bech-Nielsen G., Nord H.: *Acta Chem. Scand.* *15*, 300 (1961).
14. Nord H., Foverskov C. E., Bech-Nielsen G.: *Acta Chem. Scand.* *18*, 681 (1964).
15. Nord H., Bech-Nielsen G.: *Electrochim. Acta* *16*, 849 (1971).
16. Muralidharan V. S., Thangavel K., Balakrishnan K., Rajagopalan K. S.: *Electrochim. Acta* *29*, 1003 (1984).
17. El-Basiouny M. S., Hassan S. A., Hefny M. M.: *Corros. Sci.* *20*, 909 (1980).
18. El-Basiouny M. S., El-Kot M. S., Hefny M. M.: *Brit. Corros. J.* *14*, 51 (1979).
19. Britton H. T. S.: *Hydrogen Ions*, Vol 1. Van Nostrand, Princeton 1956.
20. Alwitt R. S.: *J. Electrochem. Soc.* *118*, 118 (1964).
21. Lewis G., Fox P. G.: *Corros. Sci.* *18*, 645 (1978).
22. Aurian-Blajeni B., Tomkiewicz M.: *J. Electrochem. Soc.* *132*, 1511 (1985).
23. Badawy W. A., El-Basiouny M. S., Ibrahim M. M.: *Indian J. Technol.* *24*, 1 (1986).
24. Graham M. J., Bardwell J. A., Goetz R., Mitchell D. F., MacDougall B.: *Corros. Sci.* *30*, 139 (1990).
25. Epelboin I., Keddam M.: *Electrochim. Acta* *17*, 177 (1972).
26. Armstrong R. D., Edmonson K., Thirsk H. R.: *Electrochim Acta* *17*, 119 (1972).
27. Mazhar A. A., Bekheet A. M., Gad-Allah A. G.: *Ann. Chem.* *71*, 471 (1984).
28. Chao C. Y., Lin L. F., MacDonald D. D.: *J. Electrochem. Soc.* *129*, 1875 (1982).
29. Hartle M., Pauli E. H.: *Electrochim. Acta* *11*, 1417 (1966).
30. Tareev B.: *Physics of Dielectric Materials*, p. 144. Mir Publishers, Moscow 1975.